Comparing Morphology and Hemodynamics of Stable-versus-Growing and Grown Intracranial Aneurysms

E.L. Leemans, B.M.W. Cornelissen, C.H. Slump, C.B.L.M. Majoie, J.R. Cebral, and H.A. Marquering

ABSTRACT

BACKGROUND AND PURPOSE: Aneurysm growth has been related to higher rupture risk. A better understanding of the characteristics related to growth may assist in the treatment decisions of unruptured intracranial aneurysms. This study aimed to identify morphologic and hemodynamic characteristics associated with aneurysm growth and to determine whether these characteristics deviate further from those of stable aneurysms after growth.

MATERIALS AND METHODS: We included 81 stable and 56 growing aneurysms. 3D vascular models were segmented on CTA, MRA, or 3D rotational angiographic images. With these models, we performed computational fluid dynamics simulations. Morphologic (size, size ratios, and shape) and hemodynamic (inflow, vorticity, shear stress, oscillatory shear index, flow instability) characteristics were automatically calculated. We compared the characteristics between aneurysms that were stable and those that had grown at baseline and final imaging. The significance level after Bonferroni correction was $P < .002$.

RESULTS: At baseline, no significant differences between aneurysms that were stable and those that had grown were detected ($P > .002$). Significant differences between aneurysms that were stable and those that had grown were seen at the final imaging for shear rate, aneurysm velocity, vorticity, and mean wall shear stress ($P < .002$). The latter was 11.5 (interquartile range, 5.4–18.8 dyne/cm^2) compared with 17.5 (interquartile range, 11.2–29.9 dyne/cm^2) in stable aneurysms ($P = .001$). Additionally, a trend toward lower area weighted average Gaussian curvature in aneurysms that had grown was observed with a median of 6.0 (interquartile range, 3.2–10.7 cm^{-2}) compared with 10.4 (interquartile range, 5.0–21.2 cm^{-2}) in stable aneurysms ($P = .004$).

CONCLUSIONS: Morphologic and hemodynamic characteristics at baseline were not associated with aneurysm growth in our population. After growth, almost all indices increase toward values associated with higher rupture risks. Therefore, we stress the importance of longitudinal imaging and repeat risk assessment in unruptured aneurysms.

ABBREVIATIONS: CFD = computational fluid dynamics; CLL = core-line length; EI = ellipticity index; ELAPSS = Earlier subarachnoid hemorrhage, location of the aneurysm, age, population, size, and shape of the aneurysm; GAA = area weighted average of the Gaussian curvature; IQR = interquartile range; LSA = low shear stress area; OSI = oscillatory shear index; PHASES = Population, Hypertension, Age, Size, Earlier Subarachnoid Hemorrhage, and Site; SizeR = size ratio; 3DRA = 3D rotational angiography; VO = mean vorticity; VOR = volume-to-ostium ratio; WSS = wall shear stress

Intracranial aneurysm rupture often leads to death or severe disability. This imposes a considerable clinical and socio-economic burden. Usually, aneurysms are asymptomatic until they rupture. Due to improvement in and the increased use of imaging, an increasing number of unruptured aneurysms are being detected.[1]

The decision to treat an unruptured aneurysm is difficult because both the treatment risk and rupture risk must be considered. Treatment risk has already been studied extensively and is dependent on the aneurysm location and size, patient age, and clinical condition; for instance, older patients have a higher risk of complications.[2,3] The most used determinants for rupture risk are size, location, and growth of the aneurysm.[4] However, many SAHs admitted to the hospital arise from small aneurysms.[5,6] Therefore, more characteristics are needed to improve the rupture risk assessment. Several additional characteristics can be derived from

Received June 20, 2019; accepted after revision September 23.

From the Departments of Biomedical Engineering and Physics (E.L.L., B.M.W.C., H.A.M.) and Radiology and Nuclear Medicine (E.L.L., B.M.W.C., C.B.L.M.M., H.A.M.), Amsterdam UMC, Academic Medical Center, University of Amsterdam, Amsterdam, the Netherlands; MIRA Institute for Biomedical Engineering and Technical Medicine (B.M.W.C., C.H.S.), University of Twente, Enschede, the Netherlands; and Bioengineering and Mechanical Engineering Department, (J.R.C.), Volgenau School of Engineering, George Mason University, Fairfax, Virginia.

This study was supported by a grant from the TWIN association, Hengelo, the Netherlands.

Please address correspondence to Eva L. Leemans, Departments of Biomedical Engineering and Physics, Radiology and Nuclear Medicine, Room L0-147, Amsterdam UMC, location AMC, Meibergdreef 9, 1105AZ, Amsterdam, the Netherlands; e-mail: e.l.leemans@amc.uva.nl

http://dx.doi.org/10.3174/ajnr.A6307

imaging data for such an assessment. These characteristics have been based on aneurysm morphology and hemodynamics.[7-9] Nevertheless, the clinical applicability of these characteristics is still limited.

Approximately 10% of aneurysms grow after detection.[10] Studies have shown a higher rupture risk in growing aneurysms.[11] As a result, aneurysm growth gives a high motivation for intervention. Yet, our understanding of the association between aneurysmal growth and rupture-related characteristics is limited. Recently, the ELAPSS score (Earlier subarachnoid hemorrhage, location of the aneurysm, age, population, size, and shape of the aneurysm) has been developed to estimate the 3- and 5-year risk of aneurysm growth.[12] This score incorporates patient characteristics (age, population, previous SAH) and aneurysm characteristics (size and location). Only a few studies have evaluated the association of more morphologic characteristics with aneurysm growth.[13-15]

Several studies have examined the relation between hemodynamics and unstable (growing or symptomatic) aneurysms.[16,17] These studies have shown a more concentrated area of high wall shear stress (WSS) with more complex intra-aneurysmal flows in unstable aneurysms. These differences have some similarities with the differences between stable and ruptured aneurysms, which show extreme high and low WSS and complex intra-aneurysmal flow patterns with a high oscillatory shear stress in ruptured aneurysms.[16,18-20]

Many of the studies evaluating the relation between hemodynamics and aneurysm stability had inconclusive findings or examined a small population. As a result, it is unknown whether aneurysm growth is associated with hemodynamic characteristics. Therefore, the primary aim of this study was to identify morphologic and hemodynamic characteristics associated with aneurysm growth. Because the rupture risk seems to increase with aneurysm growth, we also evaluated the differences between morphologic and hemodynamic characteristics of aneurysms that are stable and those that have grown at last imaging, to determine whether characteristics of aneurysms that are growing become more similar to those of ruptured aneurysms.

MATERIALS AND METHODS

Population

We combined patients from 2 data bases. The first data base consisted of all patients who presented with an unruptured intracranial aneurysm at the Amsterdam UMC, Academic Medical Center (Amsterdam), between 2012 and 2016, who had an MRA before and after aneurysm growth.

The second data base consisted of patients from multiple hospitals in the United States with an unruptured aneurysm. This data base mostly consisted of patients from the Inova Fairfax Hospital (Virginia), Mt. Sinai Medical Center (New York), and the Mayo Clinic (Minnesota). Imaging consisted of 3D rotational angiography (3DRA) or CTA. For all cases, the imaging before and after aneurysm growth was performed with the same technique.

Aneurysm growth was primarily evaluated by the local neuroradiologist. Growth was evaluated on the basis of the first and last available imaging (duration of follow-up was 0.5–13 years). Aneurysms were marked as growing when a change in size of at least 0.5 mm or a change in shape was seen. Aneurysms were marked as stable when no size or shape change was seen. Aneurysms with a total follow-up of <1 year and not showing a change in size or shape were excluded from this study. For the control group, we included all the stable cases in the second data base. Imaging of the stable cases mostly consisted of 3DRA; 10 patients had undergone CTA.

All images were anonymized. The requirement for informed consent was waived by the local institutions review boards because no diagnostics other than routine clinical imaging were used in this study.

Computational Fluid Dynamics

Computational fluid dynamics (CFD) simulations were created for all aneurysms. The first step was creating 3D vascular reconstructions. To obtain these reconstructions, we performed segmentation of the patient-specific vascular geometry and subsequently created a tetrahedral mesh. The models based on MR imaging were created with the Vascular Modeling Toolkit (www.vmtk.org; Orobix, Bergamo, Italy); the models based on CTA and 3DRA were created using in-house-developed software. The vessel segmentation extended proximally to the ICA for anterior circulation aneurysms and to the vertebral artery for posterior circulation aneurysms. In 4 cases, the vertebral artery was not present in the imaging FOV; for these cases, the segmentation started at the basilar artery.

For all cases, growth was confirmed using 3D vascular reconstructions. The models were manually aligned and evaluated for a change in size and shape. An aneurysm was definitively categorized as growing if a change of >0.5 mm was seen between baseline and last imaging.

The aneurysm was isolated by manually identifying the aneurysm neck. The position of the neck before and after growth was compared and, if needed, was corrected to make sure the positioning was comparable in both vascular reconstructions.

No patient-specific inflow conditions were available. Therefore, we used flow profiles based on phase-contrast MR imaging of healthy subjects scaled with a power law to the area of the inflow vessel.[21] Outflow boundary conditions were prescribed according to the Murray Law.[22] The CFD simulations were subsequently performed using a previously described framework.[23,24] Blood was modeled as an incompressible Newtonian fluid with a viscosity of 0.04 dyne $\times$ s/cm and a density of 1.0 g/cm^3. The vessel walls were assumed to be rigid with a nonslip boundary. For each simulation, 2 cardiac cycles were acquired. Only the last cardiac cycle was used to characterize the aneurysm hemodynamics.

Aneurysm Characteristics

We analyzed 15 previously described morphologic and 12 hemodynamic characteristics (Table 1). The morphologic characteristics were related to size (size, neck diameter, volume, and parent vessel diameter), size ratios (height-width ratio, size ratio [SizeR], aspect ratio, bulge location, volume-to-ostium ratio [VOR], and isoperimetric ratio), shape (ellipticity index [EI], nonsphericity index, undulation index, and area weighted average of Gaussian curvature [GAA]). These characteristics were calculated according to previous work.[25,26]

Table 1: Description of morphologic and hemodynamic characteristics

Name	Description	Unit
Morphologic characteristics		
Aneurysm volume	Volume of the aneurysm	cm^3
Aneurysm size	Maximum Euclidean distance of the aneurysm surface	cm
Neck size	Maximum Euclidean distance of the neck surface	cm
Parent vessel diameter	Diameter of the vessel nearest to the aneurysm neck	cm
AR	Aspect ratio; aneurysm height/neck size	Ratio
HWR	Height-to-width ratio; aneurysm height/aneurysm width	Ratio
BF	Bottleneck factor; aneurysm width/neck size	Ratio
BL	Bulge location; distance of plane with largest diameter from neck/aneurysm height	Ratio
SizeR	Size ratio	Ratio
VOR	Volume to ostium ratio; aneurysm volume/neck area	Ratio
IPR	Isoperimetric ratio; aneurysm area/aneurysm $volume^{2/3}$	Ratio
UI	Undulation index	Index
EI	Ellipticity index	Index
NSI	Nonsphericity index	Index
GAA	Area weighted average of the Gaussian curvature	cm^{-2}
Hemodynamic characteristics		
ICI	Inflow concentration index	Index
SR	Shear rate	1/s
VE	Mean velocity	cm/s
VO	Mean vorticity	1/s
WSS	Wall shear stress (time averaged mean and maximum)	$dyne/cm^2$
LSA	Low shear stress area	%
SCI	Shear concentration index	Index
OSI	Oscilatory shear index (time averaged mean and maximum)	Index
CLL	Time-averaged vortex core-line length	cm
PODE	Proper orthogonal decomposition entropy	

The determined hemodynamic characteristics were related to aneurysm inflow (inflow concentration index), intrasaccular flow (maximum velocity, mean vorticity [VO], mean shear rate, and vortex core-line length [CLL]), flow instability (proper orthogonal decomposition entropy), and aneurysm wall shear stress (maximal, mean WSS, shear concentration index, low shear area [LSA], and mean and maximum oscillatory shear index [OSI]). These characteristics were calculated according to the methods described by Mut et al.[27]

We also calculated the Population, Hypertension, Age, Size, Earlier Subarachnoid Hemorrhage, and Site (PHASES)[4] and ELAPSS[12] scores to estimate the risk of rupture and growth in the population. The PHASES score consists of the population (Finnish, Japanese, or other), the presence of hypertension, age, aneurysm size, earlier SAH, and aneurysm location. The ELAPSS score consists of earlier SAH, aneurysm location, age, population (Finnish, Japanese, or other), and aneurysm shape and size. In most patients, no data on hypertension and population were available. In these patients, zero points were awarded for the missing values.

Statistical Analysis

Normality of the data was tested using a Shapiro-Wilk test. Subsequently, normally distributed characteristics are reported as mean ± SD, and non-normally distributed characteristics, as median and interquartile range (IQR, 25%–75%).

We evaluated the difference in morphologic and hemodynamic characteristics between aneurysms that were stable and those that had grown at baseline and follow-up using an unpaired Student *t* test for normally distributed data. A Mann-Whitney *U* test was performed in case of non-normally distributed data. To prevent false discovery rates, we applied a Bonferroni correction for multiple analyses on the same dependent variable. The adjusted significance level was .002 (.05/27).

We visually compared the changes in morphology and hemodynamics during growth by evaluating the ratio between stable aneurysms and those that had grown. This ratio represents the median values of the aneurysms that had grown over the median values of the stable aneurysms.

RESULTS

We included 81 stable and 56 growing aneurysms. Patients with a growing aneurysm were more often female compared with patients with a stable aneurysm (86% compared with 65% in the stable group; $P = .004$). Patients with growing aneurysms were often younger (mean, 55 ± 14 years) compared with patients with stable aneurysms (mean, 59 ± 18 years; $P = .13$). Between the groups, there was no difference observed for aneurysm location (Table 2). Both the PHASES and ELAPSS scores did not significantly differ between aneurysms that were stable and those that had grown ($P = .05$ and .13, respectively). Growing aneurysms were significantly more frequently present in patients with a previous SAH ($P < .001$). Figure 1 shows that the basilar and posterior communicating arteries increase more in volume, compared with the MCA and ICA.

Morphology

At baseline, there were no differences in morphologic characteristics between growing and stable aneurysms. After growth, the aneurysm size and volume were slightly larger compared with stable aneurysms ($P = .006$ and $P = .006$, respectively). The SizeR showed a trend toward higher values before growth, which was significantly higher after growth (median, 1.38 [IQR,

Table 2: Baseline and hemodynamic characteristics for each group

	Stable Aneurysms	Growing Aneurysms: Baseline	Grown Aneurysms: Follow-Up Imaging
No.	81	56	56
Sex		[b]	
Male	11 (14%)	7 (12%)	
Female	53 (65%)	48 (86%)	
Unknown	17 (21%)	1 (2%)	
Artery (%)			
ACA	5 (6%)	1 (2%)	
AcomA	8 (10%)	8 (14%)	
ICA	37 (46%)	18 (32%)	
MCA	16 (20%)	19 (34%)	
PcomA	12 (15%)	3 (5%)	
Posterior circulation	3 (3%)	7 (13%)	
Previous SAH = yes (%)	2 (2%)	14 (25%)[a]	
Configuration = lateral (%)	33 (41%)	18 (32%)	
Age (mean) (SD) (yr)	59 (18)	55 (14)	59 (13)
PHASES (mean) (SD)	3 (2)	4 (3)[c]	5 (3)[a]
Without hypertension and population	3 (3)	4 (3)	5 (3)[c]
ELAPSS (mean) (SD)	14 (6)	15 (7)	17 (6)[b]
Without population	14 (6)	15 (7)	17 (6)[b]
Hemodynamic characteristics			
ICI (median) (IQR)	0.4 (0.2–1.0)	0.5 (0.3–1.2)	0.6 (0.3–1.2)
SR (median) (IQR) (1/s)	207.3 (124.0–317.5)	190.1 (67.8–273.7)	126.3 (65.1–177.0)[a]
VE (median) (IQR) (cm/s)	9.4 (5.9–13.6)	8.0 (4.6–11.4)	6.6 (3.8–10.2)[b]
VO (median) (IQR) (1/s)	270.5 (165.5–416.2)	256.9 (93.9–384.5)	177.5 (88.3–255.0)[a]
Max WSS (median) (IQR) (dyne/cm^2)	175.2 (126.8–239.2)	149.5 (107.6–194.5)[c]	146.8 (94.7–186.1)[b]
Mean WSS (median) (IQR) (dyne/cm^2)	17.5 (11.2–29.9)	16.5 (6.5–24.2)	11.5 (5.4–18.8)[a]
LSA (median) (IQR) (%)	54 (29–74)	53 (31–77)	68 (50–89)[c]
SCI (median) (IQR)	3.2 (1.9–4.6)	2.7 (1.0–4.2)	3.2 (0.2–5.7)
Max OSI (median) (IQR)	0.3 (0.1–0.4)	0.2 (0.2–0.4)	0.3 (0.2–0.4)
Mean OSI (median) (IQR)	0.01 (0.01–0.01)	0.01 (0.0–0.01)	0.01 (0.01–0.02)
CLL (median) (IQR)	0.7 (0.2–1.4)	0.6 (0.4–1.5)	1.1 (0.5–2.0)[c]
PODE (median) (IQR)	0.1 (0.1–0.2)	0.1 (0.1–0.2)	0.2 (0.1–0.3)

Note:–ACA indicates anterior cerebral artery; AcomA, anterior communicating artery; PcomA, posterior communicating artery; Q, flow rate; ICI, inflow concentration index; SR, mean aneurysm shear rate; SCI, shear concentration index; max, maximum. *P*-value compared to stable aneurysms.

[a] $P < .001$.

[b] $P < .02$.

[c] $P < .05$.

1.07–2.04] for stable aneurysms versus median, 2.14 [IQR, 1.44–3.01] for aneurysms that had grown; $P = .001$). Additionally, the GAA was slightly lower after growth with a median of 6.0 (IQR, 3.2–10.7 cm^{-2}) compared with 10.4 (IQR, 5.0–21.2 cm^{-2}) in stable aneurysms ($P = .003$). The values of all morphologic characteristics are shown in Table 3.

Hemodynamics

At baseline, there were no significant differences in hemodynamic characteristics between aneurysms that were stable and those that had grown. However, a trend toward a lower maximum WSS was seen (mean: 149.5; [IQR, 107.6–194.5 dyne/cm^2] in growing versus mean: 175.2 [IQR, 126.8–239.2 dyne/cm^2] in stable aneurysms; $P = .03$). After growth, several hemodynamic characteristics were significantly different from those in stable aneurysms: The shear rate, VO, and mean WSS were significantly lower (Table 2). For instance, median of the mean WSS was 11.5 (IQR, 5.4–18.8 dyne/cm^2) compared with 17.5 (IQR, 11.2–29.9 dyne/cm^2) in stable aneurysms ($P = .001$). Additionally, a trend was seen after growth toward a different mean intra-aneurysmal velocity, LSA, and maximum WSS between aneurysms that were stable and those that had grown.

As shown in Fig 2, after growth, most characteristics differ more from those of the stable aneurysms. Characteristics that are higher in growing than stable aneurysms at baseline increase, while characteristics that are lower at baseline decrease. There are a few exceptions: the CLL, maximum OSI, proper orthogonal decomposition entropy, and undulation index. While the OSI is slightly lower compared with stable aneurysms at baseline, it increases after growth. Similarly, the undulation index decreases.

The boxplots in Fig 3 show that the differences in some of the variables (LSA and CLL) depend on location; for instance, a much larger variation in CLL is seen in the locations with a higher risk of growth according to the ELAPSS score. The LSA shows increasingly higher values in grown aneurysms at high-risk locations for rupture and growth according to the PHASES score, while aneurysms at low-risk locations show smaller differences between aneurysms that are stable and those that have grown.

DISCUSSION

In our population, we could not identify growing aneurysms on the basis of morphologic and hemodynamic characteristics at baseline because there were minimal differences between aneurysms that were stable and those that had grown. Nevertheless, after growth, the characteristics of grown aneurysms differed more from those of stable aneurysms.

The growth rates in our study were similar to previous reported growth rates.[28] Some researchers have assumed that growth is not a continuous process but irregular and discontinuous.[29] Specific triggers might initiate aneurysm growth, such as inflammation. Therefore, the baseline images might represent aneurysms still in their stable form.

In contrast to previous studies, our study showed small differences at baseline. Previous studies have shown that growing aneurysms tend to have more complex intra-aneurysmal flow patterns at baseline with larger areas of low WSS and a more concentrated inflow.[16,17] Although we observed differences after growth, these were not seen at baseline. The smaller aneurysm

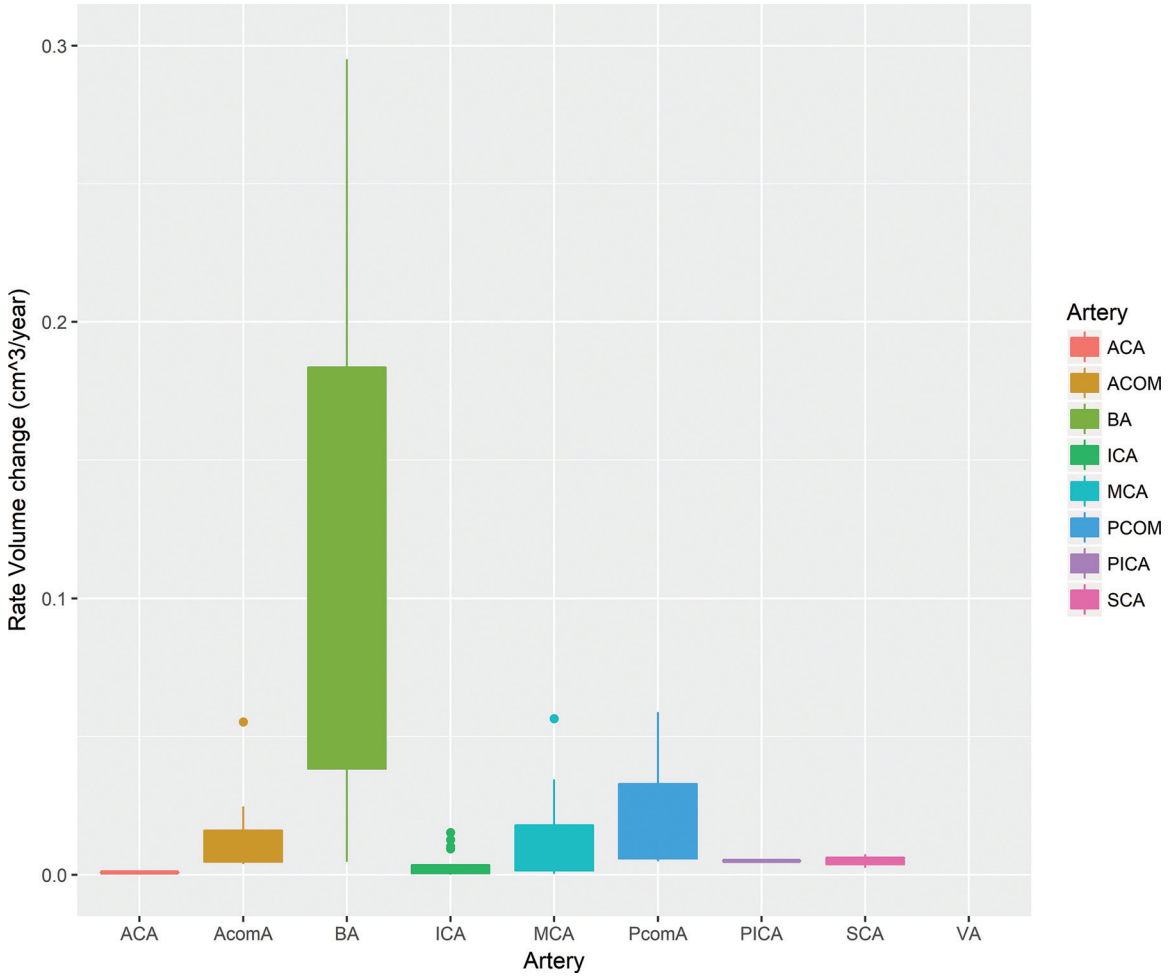

FIG 1. Boxplot showing the growth rate per aneurysm location. ACA indicates anterior cerebral artery; PcomA, posterior communicating artery; AcomA, anterior communicating artery; BA, basilar artery; SCA, superior cerebellar artery; VA, vertebral artery.

Table 3: Morphologic characteristics for each group

	Stable Aneurysms	Growing Aneurysms: Baseline	Grown Aneurysms: Follow-Up Imaging
No.	81	56	56
Aneurysm volume (median) (IQR) (cm)	0.02 (0.01–0.11)	0.03 (0.01–0.12)	0.05 (0.02–0.19)[b]
Aneurysm size (median) (IQR) (cm)	0.53 (0.36–0.76)	0.53 (0.41–0.81)	0.64 (0.46–0.97)[b]
Neck size (median) (IQR) (cm)	0.42 (0.30–0.55)	0.43 (0.33–0.62)	0.48 (0.38–0.69)[b]
Parent vessel diameter (median) (IQR) (cm)	0.37 (0.29–0.45)	0.33 (0.28–0.38)[b]	0.33 (0.28–0.38)[b]
AR (median) (IQR)	0.73 (0.53–1.10)	0.76 (0.56–0.95)	0.88 (0.71–1.08)[c]
HWR (median) (IQR)	0.82 (0.64–0.97)	0.84 (0.70–0.95)	0.90 (0.80–1.08)[b]
BF (median) (IQR)	1.00 (0.87–1.25)	1.03 (0.89–1.25)	1.15 (0.97–1.32)[c]
BL (median) (IQR)	0.30 (0.13–0.44)	0.32 (0.16–0.45)	0.39 (0.26–0.48)[b]
SizeR (median) (IQR)	0.37 (0.29–0.45)	1.82 (1.12–2.49)	2.14 (1.44–3.01)[a]
VOR (median) (IQR)	1.38 (1.07–2.04)	0.25 (0.14–0.59)	0.35 (0.20–0.89)[b]
IPR (median) (IQR)	0.22 (0.10–0.67)	4.71 (4.60–4.85)	4.71 (4.61–4.93)
UI (median) (IQR)	4.74 (4.61–4.90)	0.23 (0.14–0.36)	0.19 (0.13–0.27)
EI (median) (IQR)	0.21 (0.14–0.35)	0.26 (0.25–0.28)	0.26 (0.24–0.27)
NSI (median) (IQR)	0.26 (0.25–0.29)	0.19 (0.17–0.21)	0.19 (0.17–0.22)
GAA (median) (IQR) (cm^{-2})	10.4 (5.0–21.2)	8.7 (4.4–15.9)	6.0 (3.2–10.7)[b]

Note:—*P*-value compared with stable aneurysms.
[a] $P < .001$.
[b] $P < .02$.
[c] $P < .05$.

sizes and size ratios in our population likely result in fewer vortices and complex flow patterns.[30] Additionally, Chung et al[16] controlled for location, sex, and age. Although these did not significantly differ within our study, the location might play an important role because anterior communicating artery aneurysms might be influenced differently by the hemodynamic environment compared with MCA aneurysms. A multivariable analysis could further elucidate these differences. However, a larger sample size is needed because according to recommendations, 10–20 cases per independent variable are needed to acquire a reliable result.[31] Combining the most relevant population characteristics, the variables with a P value $< .05$, would lead to 20 independent variables, needing at least 200 patients per group. Similarly, due to the number

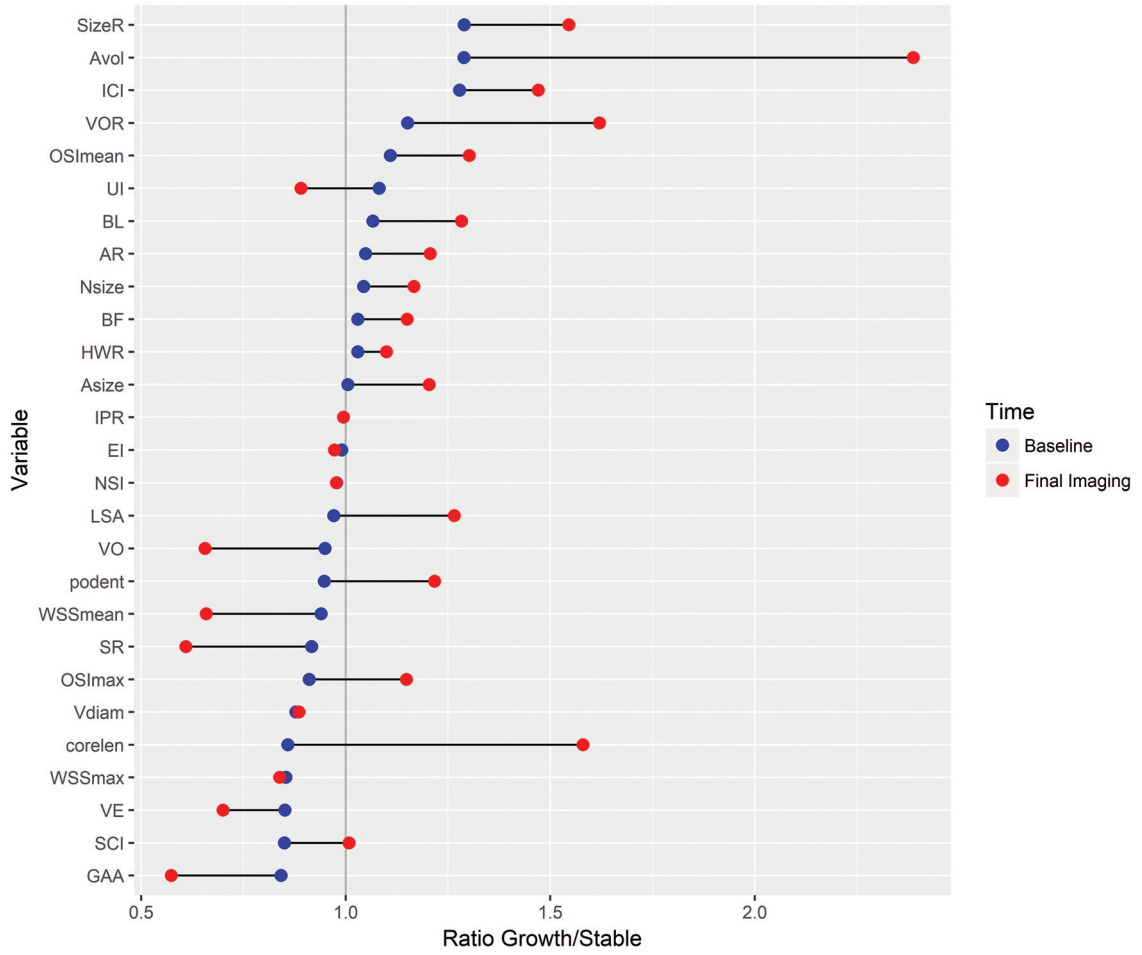

FIG 2. Dumbbell plot depicting the ratio between the median value of growing and stable aneurysms at baseline (blue) and last imaging (red). Characteristics are sorted according to baseline size. ICI indicates inflow concentration index; SR, mean aneurysm shear rate; VE, mean aneurysm velocity; SCI, shear concentration index; AR, aspect ratio; BF, bottleneck factor; BL, bulge location; IPR, isoperimetric ratio; UI, undulation index; NSI, nonsphericity index; Avol, aneurysm Volume; Nsize, Neck Size; HWR, height-to-width ratio; Asize, Aneurysm Size; podent, *proper orthogonal decomposition entropy*; max, maximum; Vdiam, Vessel diameter; corlean, core line length.

of characteristics, this study required correction for multiple testing. Larger sample sizes increase the ability to detect the differences and thus would not require such a correction.

After growth, almost all characteristics deviated further from those in stable aneurysms, indicating an association between these characteristics and instability. Additionally, several characteristics coincided with rupture-related characteristics, such as more complex flows, a lower mean WSS, a larger LSA, and viscous energy loss.[7,16,17,20,32,33] Because the hemodynamic environment is more similar to ruptured intracranial aneurysms after growth, this feature might indicate why growing aneurysms have a higher rupture risk.[11] Ruptured aneurysms have also been related to a higher maximum WSS and OSI, a trend that was not seen on follow-up imaging of the aneurysms that grew in our population. Sforza et al[17] also did not observe a significantly higher WSS and OSI in aneurysms that had gown. Therefore, it has been proposed that aneurysm growth occurs at regions of low WSS.[18,34] We observed a trend toward larger areas of low WSS after growth; however, this trend seems significant in high-risk locations for growth and rupture (communicating arteries and posterior circulation). Therefore, although similarities in the hemodynamic environment exist between aneurysms that have ruptured and those that have grown, the differences might show different underlying mechanisms between growth and rupture. A low wall shear stress is associated with inflammation and atherosclerosis, while high shear stresses are associated with mural cell destruction and flow impingment.[18] Thus low shear stresses likely cause aneurysms to remodel and repair, while high shear stresses causes the wall to degenerate and rupture.

The PHASES score has been developed to predict rupture,[4] and more recently, it has also been shown to be associated with aneurysm growth.[35] Consistent with these studies, the growing aneurysms in our study showed higher PHASES scores at baseline. Nevertheless, the baseline ELAPSS scores—developed to predict growth[12]—did not significantly differ between growing and stable aneurysms in our study. The main differences between these scores is that the ELAPSS includes irregularity and has different weights for the prediction model for location and size. Our presented population had similar sizes, ages, and irregularity at baseline for growing and stable aneurysms, which likely resulted in similar ELAPSS scores.

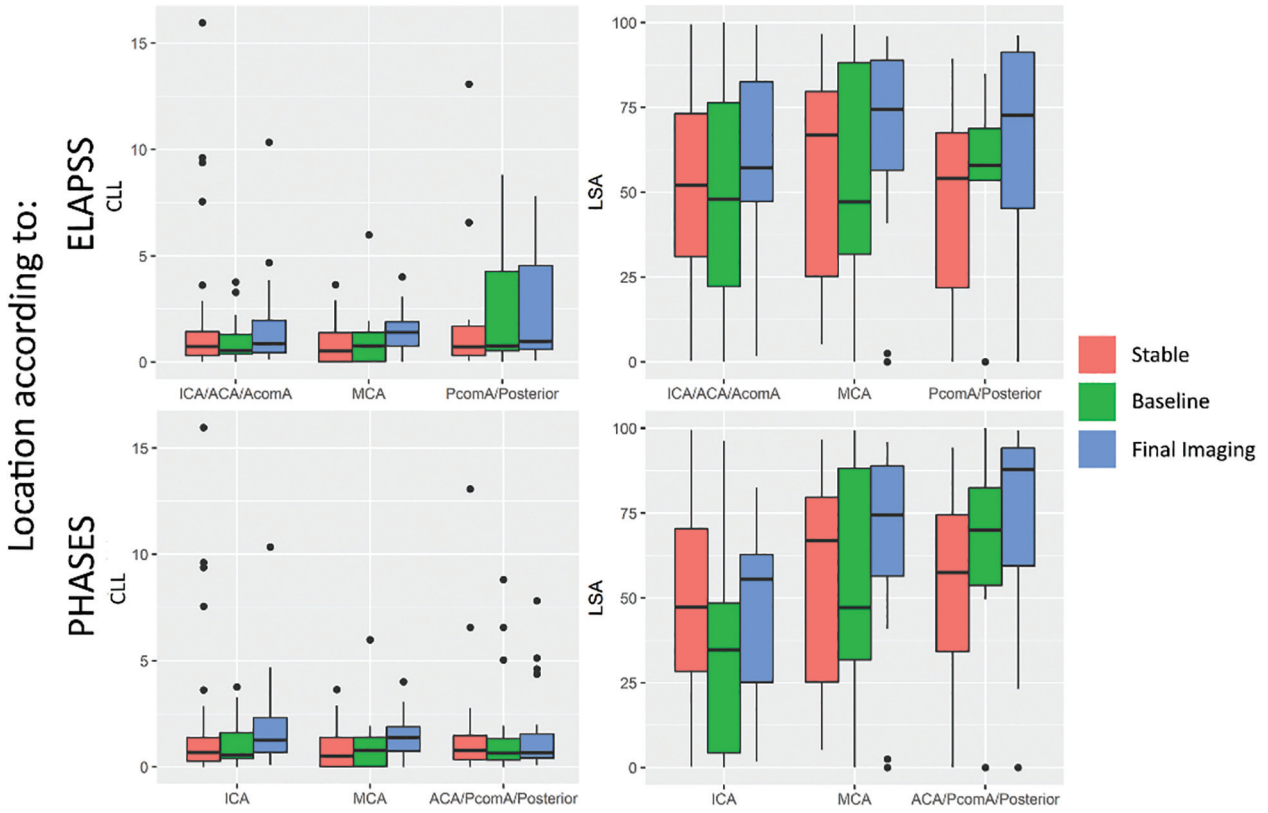

FIG 3. Boxplot comparing core-line length (*left*) and low shear area (*right*) in the different location categories according to the ELAPSS (*upper row*) and PHASES (*lower row)* scores. ACA indicates anterior cerebral artery; PcomA, posterior communicating artery; AcomA, anterior communicating artery.

This study has several limitations. First, a selection bias is present because this study only included aneurysms with longitudinal data. Therefore, the aneurysms in this study likely had a low rupture risk because aneurysms considered to be at high risk are treated at a short notice. However, the presented cases do give information on the course of untreated aneurysms. Additionally, due to the limited resolution of the CTA and MRA images (approximately 0.5 mm), some cases with little growth (<0.5 mm) might be missed. Most studies of aneurysm growth only assess growth >0.5 or 1 mm.[12,15] Therefore, this study also had 0.5 mm as a lower limit for growth.

Second, the accuracy of the CFD model is highly dependent on the segmentations. This study used multiple imaging methods to acquire all the patient-specific segmentations. To optimize the comparability between baseline and follow-up imaging of growing aneurysms, the same imaging technique was used for both time points. All segmentations were visually inspected and corrected to make sure inflow and outflow vessels were similar in size at both time points. The vascular models of stable cases were mostly based on 3DRA, while CTA and MRA were used for growing aneurysms. Because 3DRA is an invasive method, it is not often used in follow-up imaging, resulting in the differences among groups. Every imaging technique has some systematic errors;[36] as a result, each segmentation method was tailored to the imaging technique. Differences between techniques were minimized by manually checking and correcting each segmentation. However, we observed slight-but-insignificant lower parent vessel diameters in growing aneurysms, especially in the MRA images. These differences could reflect actual size differences but are more likely due to the different imaging resolutions and methods. Previous studies have reported similar differences between imaging modalities; comparing time-of-flight MRA with digital subtraction angiography has shown smaller diameters in the MRA images.[37-39] This systematic error could influence differences between aneurysms that were stable and those that had grown, leading to lower flow conditions in growing aneurysms because these were mostly imaged with MRA.

Additionally, the CFD models are based on several assumptions and approximations about intra-aneurysmal flow and resulting hemodynamic characteristics. For instance, because no patient-specific flow conditions were available, we used typical flow waveforms derived from healthy volunteers. Previous studies have shown that the patient-specific inflows and the completeness of the circle of Willis could significantly influence the inflow rates.[40,41] For instance, lower basilar flow rates were observed with hypoplastic or absent P1 arteries. For anterior communicating artery aneurysms, we imposed flow conditions at both ICAs; thus, the effect of a hypoplastic or absent A1 segment was included into the model. However, we did not take into account the influence of a hypoplastic or absent P1. Only a small proportion of the patients in our dataset had a posterior aneurysm, and because the P1 was missing in only some patients, it is expected that the change in inflow had a minor influence on the presented results.

CONCLUSIONS

No association was found between morphologic and hemodynamic characteristics and aneurysm growth at baseline. However, after growth, the differences in morphology and hemodynamics between aneurysms that have grown and those that are stable increased. Therefore, aneurysms that have grown likely have a higher rupture risk.

Disclosures: Eva L. Leemans—*RELATED*: *Grant/Grants Pending*: TWIN association, *Comments*: This study was supported by a grant from the TWIN association, Hengelo, the Netherlands.* Bart M.W. Cornelissen—*RELATED*: *Grant/Grants Pending*: TWIN association.* Charles B.L.M. Majoie—*RELATED*: *Grant/Grants Pending*: TWIN association,* the Dutch Heart Foundation,* and Stryker.* *OTHER*: cofounder of and shareholder in Nico-lab. Juan R. Cebral—*RELATED*: *Grant/Grants Pending*: National Institutes of Health,* *UNRELATED*: *Grant/Grants Pending*: National Institutes of Health/Philips, *Comments*: research grants.* Henk A. Marquering—*RELATED*: *Grant/Grants Pending*: TWIN association; *OTHER*: cofounder of and shareholder in Nico-lab. Cornelis H. Slump—*RELATED*: *Grant/Grants Pending*: TWIN association. *Money paid to the institution.

REFERENCES

1. Gabriel RA, Kim H, Sidney S, et al. **Ten-year detection rate of brain arteriovenous malformations in a large, multiethnic, defined population.** *Stroke* 2010;41:21–26 CrossRef Medline
2. Lecler A, Raymond J, Rodriguez-Régent C, et al. **Intracranial aneurysms: recurrences more than 10 years after endovascular treatment: a prospective cohort study.** *Radiology* 2015;277:173–80 CrossRef Medline
3. Molyneux AJ, Birks J, Clarke A, et al. **The durability of endovascular coiling versus neurosurgical clipping of ruptured cerebral aneurysms: 18-year follow-up of the UK cohort of the International Subarachnoid Aneurysm Trial (ISAT).** *Lancet* 2015;385:691–97 CrossRef Medline
4. Greving JP, Wermer MJH, Brown RD, et al. **Development of the PHASES score for prediction of risk of rupture of intracranial aneurysms: a pooled analysis of six prospective cohort studies.** *Lancet Neurol* 2014;13:59–66 CrossRef Medline
5. Weir B, Disney L, Karrison T. **Sizes of ruptured and unruptured aneurysms in relation to their sites and the ages of patients.** *J Neurosurg* 2002;96:64–70 CrossRef Medline
6. Korja M, Kaprio J. **Controversies in epidemiology of intracranial aneurysms and SAH.** *Nat Rev Neurol* 2016;12:50–55 CrossRef Medline
7. Xiang J, Natarajan SK, Tremmel M, et al. **Hemodynamic-morphologic discriminants for intracranial aneurysm rupture.** *Stroke* 2011;42:144–152 CrossRef Medline
8. Cebral JR, Mut F, Weir J, et al. **Quantitative characterization of the hemodynamic environment in ruptured and unruptured brain aneurysms.** *AJNR Am J Neuroradiol* 2011;32:145–51 CrossRef Medline
9. Dhar S, Tremmel M, Mocco J, et al. **Morphology parameters for intracranial aneurysm rupture risk assessment.** *Neurosurgery* 2008;63:185–97 CrossRef Medline
10. Etminan N, Rinkel GJ. **Unruptured intracranial aneurysms: development, rupture and preventive management.** *Nat Rev Neurol* 2016;12:699 CrossRef Medline
11. Villablanca JP, Duckwiler GR, Jahan R, et al. **Natural history of asymptomatic unruptured cerebral aneurysms evaluated at CT angiography: growth and rupture incidence and correlation with epidemiologic risk factors.** *Radiology* 2013;269:258–65 CrossRef Medline
12. Backes D, Rinkel GJE, Greving JP, et al. **ELAPSS score for prediction of risk of growth of unruptured intracranial aneurysms.** *Neurology* 2017;88:1600–06 CrossRef Medline
13. Chien A, Xu M, Yokota H, et al. **Nonsphericity index and size ratio identify morphologic differences between growing and stable aneurysms in a longitudinal study of 93 cases.** *AJNR Am J Neuroradiol* 2018;39:500–06 CrossRef Medline
14. Ramachandran M, Raghavan ML. *On the Role of Intracranial Aneurysm Morphology in Stable versus Unstable Lesions*. Iowa City: University of Iowa; 2012
15. Backes D, Rinkel GJ, Laban KG, et al. **Patient- and aneurysm-specific risk factors for intracranial aneurysm growth: a systematic review and meta-analysis.** *Stroke* 2016;47:951–57 CrossRef Medline
16. Chung BJ, Mut F, Putman CM, et al. **Identification of hostile hemodynamics and geometries of cerebral aneurysms: a case-control study.** *AJNR Am J Neuroradiol* 2018;39:1860–66 CrossRef Medline
17. Sforza DM, Kono K, Tateshima S, et al. **Hemodynamics in growing and stable cerebral aneurysms.** *J Neurointerv Surg* 2016;8:407–12 CrossRef Medline
18. Meng H, Tutino VM, Xiang J, et al. **High WSS or low WSS? Complex interactions of hemodynamics with intracranial aneurysm initiation, growth, and rupture: toward a unifying hypothesis.** *AJNR Am J Neuroradiol* 2014;35:1254–62 CrossRef Medline
19. Fan J, Wang Y, Liu J, et al. **Morphological-hemodynamic characteristics of intracranial bifurcation mirror aneurysms.** *World Neurosurg* 2015;84:114–120.e2 CrossRef Medline
20. Doddasomayajula R, Chung BJ, Mut F, et al. **Hemodynamic characteristics of ruptured and unruptured multiple aneurysms at mirror and ipsilateral locations.** *AJNR Am J Neuroradiol* 2017;38:2301–07 CrossRef Medline
21. Cebral JR, Castro MA, Putman CM, et al. **Flow-area relationship in internal carotid and vertebral arteries.** *Physiol Meas* 2008;29:585–94 CrossRef Medline
22. Murray CD. **The physiological principle of minimum work, I: the vascular system and the cost of blood volume.** *Proc Natl Acad Sci U S A* 1926;12:207–14 CrossRef Medline
23. Cebral JR, Castro M, Burgess JE, et al. **Characterization of cerebral aneurysms for assessing risk of rupture by using patient-specific computational hemodynamics models.** *AJNR Am J Neuroradiol* 2005;26:2550–59 Medline
24. Cebral JR, Mut F, Sforza D, et al. **Clinical application of image-based CFD for cerebral aneurysms.** *Int J Numer Method Biomed Eng* 2011;27:977–92 CrossRef Medline
25. Raghavan ML, Ma B, Harbaugh RE. **Quantified aneurysm shape and rupture risk.** *J Neurosurg* 2005;102:355–62 CrossRef Medline
26. Ma B, Harbaugh RE, Raghavan ML. **Three-dimensional geometrical characterization of cerebral aneurysms.** *Ann Biomed Eng* 2004;32:264–73 CrossRef Medline
27. Mut F, Löhner R, Chien A, et al. **Computational hemodynamics framework for the analysis of cerebral aneurysms.** *Int J Numer Method Biomed Eng* 2011;27:822–39 CrossRef Medline
28. Jou LD, Mawad ME. **Growth rate and rupture rate of unruptured intracranial aneurysms: a population approach.** *Biomed Eng Online* 2009;8:1–9 CrossRef Medline
29. Koffijberg H, Buskens E, Algra A, et al. **Growth rates of intracranial aneurysms: exploring constancy.** *J Neurosurg* 2008;109:176–85 CrossRef Medline
30. Tremmel M, Dhar S, Levy EI, et al. **Influence of intracranial aneurysm-to-parent vessel size ratio on hemodynamics and implication for rupture: results from a virtual experimental study.** *Neurosurgery* 2009;64:622–30; discussion 630–31 CrossRef Medline
31. Tabachnick BG, Fidell LS. *Using Multivariate Statistics*. 6th ed. New York: Pearson; 2013
32. Varble N, Rajabzadeh-Oghaz H, Wang J, et al. **Differences in morphologic and hemodynamic characteristics for "PHASES-based" intracranial aneurysm locations.** *AJNR Am J Neuroradiol* 2017;38:2105–10 CrossRef Medline
33. Xu J, Yu Y, Wu X, et al. **Morphological and hemodynamic analysis of mirror posterior communicating artery aneurysms.** *PLoS One* 2013;8:e55413 CrossRef Medline
34. Boussel L, Rayz V, McCulloch C, et al. **Aneurysm growth occurs at region of low wall shear stress: patient-specific correlation of**

hemodynamics and growth in a longitudinal study. *Stroke* 2008; 39:2997–3002 CrossRef Medline

35. Backes D, Vergouwen MD, Groenestege AT, et al. **PHASES score for prediction of intracranial aneurysm growth.** *Stroke* 2015;46:1221–27 CrossRef Medline
36. Schneiders JJ, Marquering HA, Antiga L, et al. **Intracranial aneurysm neck size overestimation with 3D rotational angiography: the impact on intra-aneurysmal hemodynamics simulated with computational fluid dynamics.** *AJNR Am J Neuroradiol* 2013;34:121–28 CrossRef Medline
37. Behme D, Amelung N, Khakzad T, et al. **How to size intracranial aneurysms: a phantom study of invasive and noninvasive methods.** *AJNR Am J Neuroradiol* 2018: 39:2291–96 CrossRef Medline
38. Lauric A, Hippelheuser JE, Malek AM. **Critical role of angiographic acquisition modality and reconstruction on morphometric and haemodynamic analysis of intracranial aneurysms.** *J Neurointerv Surg* 2018;10:911–15 CrossRef Medline
39. Millán RD, Dempere-Marco L, Pozo JM, et al. **Morphological characterization of intracranial aneurysms using 3-D moment invariants.** *IEEE Trans Med Imaging* 2007;26:1270–82 CrossRef Medline
40. Cornelissen BMW, Schneiders JJ, Sprengers ME, et al. **Aneurysmal parent artery-specific inflow conditions for complete and incomplete circle of Willis configurations.** *AJNR Am J Neuroradiol* 2018;39:910–15 CrossRef Medline
41. Jansen IG, Schneiders JJ, Potters WV, et al. **Generalized versus patient-specific inflow boundary conditions in computational fluid dynamics simulations of cerebral aneurysmal hemodynamics.** *AJNR Am J Neuroradiol* 2014;35:1543–48 CrossRef Medline